Ablation Pressure Driven by an Energetic Electron Beam in a Dense Plasma

S. Gus'kov, X. Ribeyre, M. Touati, J.-L. Feugeas, Ph. Nicolaï, V. Tikhonchuk

▶ **To cite this version:**

S. Gus'kov, X. Ribeyre, M. Touati, J.-L. Feugeas, Ph. Nicolaï, et al.. Ablation Pressure Driven by an Energetic Electron Beam in a Dense Plasma. Physical Review Letters, 2012, 109 (25), pp.255004. 10.1103/PhysRevLett.109.255004 . hal-04394389

HAL Id: hal-04394389
https://hal.science/hal-04394389v1

Submitted on 15 Jan 2024

HAL is a multi-disciplinary open access archive for the deposit and dissemination of scientific research documents, whether they are published or not. The documents may come from teaching and research institutions in France or abroad, or from public or private research centers.

L'archive ouverte pluridisciplinaire **HAL**, est destinée au dépôt et à la diffusion de documents scientifiques de niveau recherche, publiés ou non, émanant des établissements d'enseignement et de recherche français ou étrangers, des laboratoires publics ou privés.

Ablation Pressure Driven by an Energetic Electron Beam in a Dense Plasma

S. Gus'kov,[1,2] X. Ribeyre,[2,*] M. Touati,[2] J.-L. Feugeas,[2] Ph. Nicolaï,[2] and V. Tikhonchuk[2]

[1]*P. N. Lebedev Physical Institute, RAS, Leninskii Prospect 53, Moscow 119991, Russia*

[2]*Université Bordeaux-CNRS-CEA, Centre Lasers Intenses et Applications, UMR 5107, 33405 Talence, France*

(Received 8 September 2012; published 19 December 2012)

An intense beam of high energy electrons may create extremely high pressures in solid density materials. An analytical model of ablation pressure formation and shock wave propagation driven by an energetic electron beam is developed and confirmed with numerical simulations. In application to the shock-ignition approach in inertial confinement fusion, the energy transfer by fast electrons may be a dominant mechanism of creation of the igniting shock wave. An electron beam with an energy of 30 keV and energy flux 2–5 PW/cm^2 can create a pressure amplitude more than 300 Mbar for a duration of 200–300 ps in a precompressed solid material.

DOI: 10.1103/PhysRevLett.109.255004 PACS numbers: 52.50.Jm, 52.35.Tc, 52.72.+v, 98.38.Fs

Energetic electrons are commonly considered a dangerous effect for inertial confinement fusion (ICF). Having a long mean free path, they penetrate through the solid shell and depose their energy in the ablator and deuterium-tritium fuel. That effect significantly increases the target entropy, thus preventing it from efficient implosion. The phenomenon of target preheat was the major reason for several milestone events [1]: cessation of the ICF program based on the CO_2 laser in the 1980s, switching to the third harmonic in the Nd:glass ICF lasers, and limiting the "useful" laser intensities to a few PW/cm^2. All these limitations significantly reduce the ICF operational domain. However, matching the mean free path of fast electrons with the target size may suppress the negative effect of preheat and open the possibility of using the energetic particles for creation of a high ablation pressure [2–4]. Fast ignition is an example of the application of energetic electrons in ICF. Here, a beam of relativistic electrons is supposed to create a small hot spot in the compressed fuel [5]. This scheme, nevertheless, faces serious difficulties related to tight focusing of an intense electron beam.

Energetic electrons may play an important role in the creation of a high ablation pressure, which is interesting for ignition of fusion reactions in the laboratory [6,7] and in astrophysics [8,9]. In the shock ignition scheme in inertial confinement fusion, the fuel is ignited by a strong shock launched by an intense laser spike at the end of the implosion process. The laser spike intensity is in the range of 10 PW/cm^2, certainly well above the threshold of parametric instabilities, and a significant part of laser energy is expected to be deposited in the nonthermal, energetic electrons [10,11]. It was suggested [7,12] that their deleterious effect on target implosion can be mitigated by the fact that at the moment of spike arrival the target has already passed halfway through the implosion phase, and its areal density is increased significantly, by a factor of 10–20 at least. If the target areal density would be larger than the range of fast electrons, the latter will be stopped in the imploding shell and may play a positive role by contributing to the ablation pressure.

There is no general model of pressure formation by an energetic particle beam. The models [3] apply for nanosecond electron beams where the thermal electron heat conductivity plays an important role. In this case, the laser energy is deposited at the critical density and it is transported to the ablation zone by the thermal electrons. This is a stationary ablation process where the shock wave launched into the solid material is connected to the isothermal rarefaction wave [13–15], as it is schematically shown in Fig. 1(a). Ablation by an energetic ion beam was considered in Ref. [4]. A recent paper [16] considers the regime of transition from the thermal electron diffusion to a nonlocal energy transport. However, the fast electron plasma heating is limited to a very short time scale, before the hydrodynamic separation takes place. It is not sufficient for description of the shock wave amplitude and its temporal evolution.

In this Letter, for the first time, we propose a model of dense target heating by a beam of energetic electrons and the shock pressure formation. The fast electrons, similarly to energetic x rays, propagate deeper in the target behind the ablation front created by the thermal electron conduction and produce a second ablation front. However, different from x rays and thermal electrons, the range of fast electrons

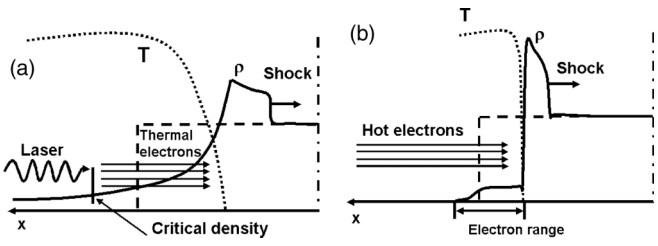

FIG. 1. Density and temperature profiles in the stationary laser ablation regime (a) and in the hot electron beam ablation nonstationary regime after the loading time (b).

 © 2012 American Physical Society

does not depend on the plasma temperature. For this simple reason, the standard stationary isothermal model of plasma expansion does not apply to fast electrons. The fast electron ablation is intrinsically a nonstationary process similar to the ion driven ablation [4]. It can be described by a model of ablation of a finite mass that depends on the fast electron range. Consequently, the shock is launched by the ablation pressure created by fast electrons during a finite time interval, the loading time, and after that the shock amplitude decreases slowly with time. Figure 1(b) presents schematically the density and temperature profiles in this regime after the loading time. Thus, the fixed energy deposition range of fast particles implies an existence of an optimal time for fast electron beam injection: shorter beams will drive a smaller amplitude shock, while longer beams will be detached from the solid target and depose their energy in the expanding plasma, thus decreasing the coupling efficiency.

The fast electron ablation theoretical model is presented here for a simple case of monoenergetic electrons and a plane geometry. Its validity is confirmed with hydrodynamic simulations where the fast electron transport is described by a reduced kinetic model.

There are two classes of self-similar solutions of equations of ideal hydrodynamics that describe a rarefaction wave. One of them is the well-known stationary isothermal rarefaction wave, where the temperature is constant and the ablated mass increases linearly with time [13–15]. Another one describes an isothermal expansion of a given mass plasma with a temperature increasing with time [17,18]. The isothermal model applies readily to the energy deposition of laser beams and thermal x rays [15,19]. There the plasma temperature is adjusted in a way that it accommodates the photon stopping length to the plasma density profile. This model, however, does not apply to fast electrons because their stopping power depends only on the fast electron energy ε_{e0}. An electron beam deposes all its energy over the distance

$$x_h = 4\pi\psi\epsilon_0^2\varepsilon_{e0}^2/e^4 n_e \ln\Lambda,$$

where n_e is the electron density, e is the elementary charge, $\ln\Lambda$ is the Coulomb logarithm, and ψ is a numerical factor accounting for the electron-ion scattering. (For simplicity, we consider nonrelativistic electrons.) For a fully ionized deuterium-tritium plasma with density of 10 g/cm^3, the stopping length of a beam of collimated electrons is 1.8 μm for the electron energy 30 keV and 15 μm for $\varepsilon_{e0} = 100$ keV. Correspondingly, the heated areal mass $\rho_0 x_h$, where ρ_0 is the initial target density, depends only on the initial electron energy. Moreover, as the fast electron range does not depend on plasma temperature, the electron beam will depose its energy in the same mass even when this mass expands.

This reasoning enables us to introduce the following two-stage model of plasma expansion driven by a monoenergetic electron beam transporting the energy flux $I_b = n_b\varepsilon_{e0}v_{e0}$, where $v_{e0} = (2\varepsilon_{e0}/m_e)^{1/2}$ is the initial electron velocity. At the first stage, the plasma is heated by the incident beam of fast electrons and starts expanding. The plasma energy increases linearly with time. It is redistributed between the internal energy, $W_{\rm int} = (3/2)\int \rho_0 c_s^2 dx$, where $c_s = (ZT/m_i)^{1/2}$ is the acoustic velocity, and the kinetic energy of expanding plasma, $W_{\rm kin} = (1/2)\int \rho_0 u^2 dx$:

$$W_{\rm int} + W_{\rm kin} = I_b t. \tag{1}$$

The repartition between the internal and kinetic energies in the heated layer, $W_{\rm kin}/W_{\rm int} = \zeta(t)$, increases with time. The duration of this stage, the loading time, t_h, is defined by the time of propagation of the rarefaction wave across the heated layer, $t_h \simeq x_h/c_{sh}$. The coefficient ζ can be evaluated by requesting a continuity of the plasma density and pressure at the time t_h with the self-similar solution. At the expansion phase, the absorbed energy is equally divided between the kinetic and internal energy. Thus, $\zeta(t_{th}) = 1$, and the loading time and the pressure at this stage read:

$$t_h = (9/2\pi)^{1/3} x_h/D_0, \qquad p_m = p_h t/t_h, \tag{2}$$

where $p_h = (6\pi)^{-1/3} I_b/D_0$ is the maximum pressure and $D_0 = (I_b/\rho_0)^{1/3}$ is the characteristic hydrodynamic velocity. Note that the maximum pressure depends only on the beam intensity and on the target density, while the loading time increases strongly with the electron energy in agreement with Ref. [4]. For electron beam intensities in the range of PW/cm^2, the heating proceeds so fast that the electron thermal conduction does not play a significant role, and the heated mass undergoes expansion without transferring the internal energy to adjacent cold plasma. However, the pressure in the heated layer exercises a mechanical work and launches a shock wave in the cold plasma.

Expansion of a heated layer of plasma continuously heated by an electron beam is described by the isothermal rarefaction wave of a constant mass [17]. It corresponds to the following self-similar solution of ideal hydrodynamics equations:

$$u = \frac{3(x - x_h)}{2t}, \qquad T = \frac{m_i I_b t}{3(Z+1)\rho_0 x_h},$$
$$\rho = \frac{3(\rho_0 x_h)^{3/2}}{\sqrt{2\pi I_b} t^{3/2}} \exp\left(-\frac{9\rho_0 x_h (x_h - x)^2}{8 I_b t^3}\right). \tag{3}$$

Here, the velocity increases linearly with the coordinate for $x < x_h$, the temperature increases linearly with time, and the density profile has a Gaussian-like shape with the characteristic scale length $L_\rho = (2D_0 t)^{3/2}/3x_h^{1/2}$, increasing with time as $t^{3/2}$. As this self-similar solution corresponds to an infinitely thin initial heated layer, it formally diverges at $t = 0$, but it has a physical sense for times longer than the loading time t_h.

The effect of expanding plasma on the shock wave formation depends on the values of plasma density and pressure at the cold plasma interface at $x = x_h$:

$$\rho_m = \rho_0 (t_h/t)^{3/2}, \qquad p_m = p_h (t_h/t)^{1/2}. \tag{4}$$

The latter decreases as a square root of time. As an example, we consider an electron beam with energy $\varepsilon_{e0} = 30$ keV and intensity $I_b = 1$ PW/cm^2 incident on a deuterium-tritium plasma with density 10 g/cm^3. Then the maximum pressure p_h rises to the value of 380 Mbar. The loading time is relatively short, $t_h \simeq 20$ ps. However, for longer times, the pressure decreases rather slowly.

Knowing the pressure, it is straightforward to evaluate the energy invested in the shock. It is described by the mechanical work $\mathcal{E}_{sh} = (3/4) \int_0^t p_m D_{sh} dt$, where $D_{sh} = (4p_m/3\rho_0)^{1/2}$ is the shock wave velocity in the strong pressure limit [20,21]. Then the efficiency of the shock drive is a ratio of $\mathcal{E}_{sh}$ to the injected electron beam energy $\mathcal{E}_b = I_b t$. During the loading time, $t < t_h$, the shock energy increases as $t^{5/2}$, achieving the value of $(1/5)\,(2\pi)^{-1/2} I_b t_h$ at $t = t_h$. After that time the shock energy is increasing much slower as $t^{1/4}$. Consequently, the maximum efficiency of the shock excitation by an electron beam is achieved if the beam duration is twice the loading time, $t_m \simeq 2t_h$. At that particular moment, the coupling efficiency is $\eta_{\max} = \mathcal{E}_{sh}(t_m)/I_b t_m \approx 0.115$, and it decreases with time very slowly for $t > t_m$. Even for $t = 10t_h$, the coupling efficiency is reduced from the maximum value only by 12%. Therefore, the electron beams of a duration of a few hundred picoseconds could drive high amplitude hydrodynamic shocks efficiently.

The limits of the present model are threefold. First, the target thickness, obviously, should be larger than the electron beam stopping length. In practice, having in mind the electron energies of several tens of keV and the stopping lengths x_h of a few microns, the target density needs to be in the range of 10 g/cm^3 or more. Second, the planar model is limited by the two-dimensional effects. Thus, the thickness of the expanding plasma layer, $\Delta x \simeq (D_0 t)^{3/2} x_h^{-1/2}$, according to Eq. (3), should be smaller than the characteristic distance in the second dimension R (the shell radius for a spherical target or the electron beam radius for a planar target). This condition limits the time to $t < t_h (R/x_h)^{2/3}$. Considering the shell radius of 200 μm, this condition allows the time intervals of a few hundred ps in the examples discussed above. Third, a strong plane shock may become unstable with respect to front modulations if the target is accelerated. However, this effect needs a global description of the target dynamics, which is out of the scope of this Letter.

The theoretical model of a shock driven by an energetic electron beam has been compared with the hydrodynamic simulations conducted with the code CHIC [22]. This code is currently used to simulate laser-plasma interaction experiments. It includes thermal coupling of electrons and ions, classical or nonlocal electron heat conduction, and a detailed radiation transport with the tabulated ionization and the opacity data. For comparison with the model, we use here a one-dimensional plane version of the code complemented with a kinetic module $M1$ describing a transport of fast electrons in plasma [23].

This fast kinetic module describes the electron transport in the ion reference frame by solving the equations for two angular moments of the relativistic Fokker-Planck equation with a specific entropy closure relation that accounts for the angular width of the electron beam [24]. It takes into account the electron collisional slowing down on the plasma free electrons, bound electrons, plasmons, and the elastic scattering on ions. The collective effects are also taken into account through the self-consisted electric field. The latter is calculated assuming that the return current fully compensates the beam current.

At the initial time, a deuterium-tritium plasma has a steplike profile with the maximum density $\rho_0 = 10$ g/cm^3 and the temperature of 1 eV. The plasma thickness of 100 μm is much larger than the fast electron range, thus allowing us to observe the creation and propagation of the shock wave for a sufficiently long time of the order of 1 ns. The intensity of a monoenergetic, collimated electron beam was maintained constant in time. Two representative cases with $I_b = 1$ PW/cm^2 and $\varepsilon_{e0} = 30$ keV (case 1) and $I_b = 10$ PW/cm^2 and $\varepsilon_{e0} = 100$ keV (case 2) have been tested. In both cases, because of high plasma density, the resistive losses are small and the electron energy deposition is due to the collisional effects.

Figure 2 shows the plasma pressure and density profiles for case 1. The mean free path of fast electrons is initially of

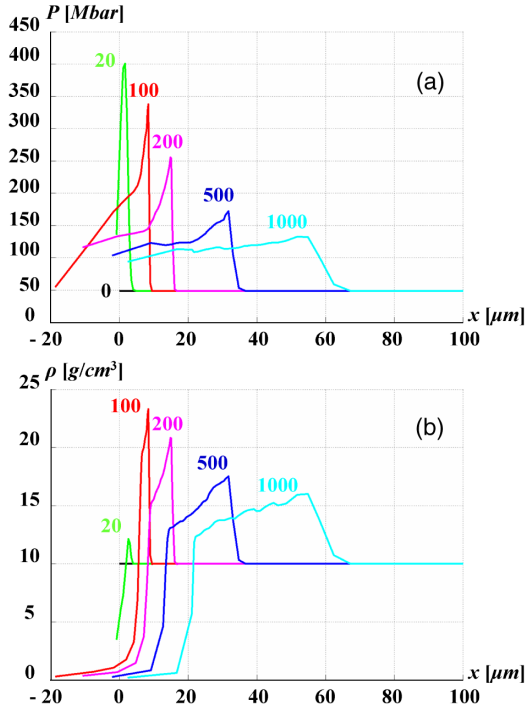

FIG. 2 (color online). Snapshots of distributions of the plasma pressure (a) and the density (b). The numbers near the curves indicate the time in picoseconds. The electron beam energy is 30 keV and the intensity is 1 PW/cm^2.

the order of 2 μm, the characteristic hydrodynamic velocity is $D_0 = 100$ μm/ns, and the corresponding loading time (2) is 20 ps. According to the theoretical previsions, the maximum pressure p_h rises to 400 Mbar at the loading time $t_h \simeq 20$ ps, and the density increases by a factor of 2.7 after the loading time. Then, as time goes on, the pressure drops down to $p_{sh} \simeq 120$ Mbar, and the shock takes a triangular shape characteristic for a blast wave. It propagates with a velocity $D_{sh} \simeq 60$ μm/ns. Consequently, the shock wave power $P_{sh} = p_{sh} D_{sh}$ is about 70 TW/cm^2. That corresponds to the driver efficiency of 7%, which agrees well with the maximum theoretical value of ~10%.

The fast electron energy deposition does not move along with the shock front, but instead moves out and spreads over the expanding plasma. The front edge of the energy deposition zone coincides with the rear edge of the density compression. Thus, the deposited energy becomes decoupled from the shock, so the shock pressure drops down with time. Comparison of the runs with and without electron thermal conductivity shows that its role is negligible at the loading stage as the plasma temperature in the shock is rather low, just a few eV. Later in time, after ~600 ps, the thermal wave from the hot corona catches up to the shock and broadens the pressure profile.

The electron beams of higher energy and intensity may create even much stronger blast waves. For case 2 shown in Fig. 3, the loading time is ~80 ps and the shock pressure rises to 1800 Mbar at the time of 100 ps. It reduces then to 700 Mbar after 1 ns. The shock velocity is about 120 μm/ns and the shock power is about 0.7 PW/cm^2. The Gaussian-like density profile corresponding to the self-similar solution (3) with $L_\rho = 20$ μm for $t = 100$ ps is shown in Fig. 3(b) with a dashed line. It agrees rather well with the numerical solution shown with a red line corresponding to the time of 100 ps. The density profile in the shock in the later time, $t > 200$ ps, takes a two-humps shape. The second hump is driven by the thermal wave catching up to the shock at the time of 1 ns. The driving efficiency of the beam remains at the same level of 7% as in case 1.

Theoretical analysis of the fast electron driven shock wave in dense solids, confirmed by numerical simulations, shows a possibility to achieve extremely high shock pressures in high density solid materials with the coupling efficiency up to 10%. The major condition is that target areal densities should be of a few tenths of g/cm^2 or more, higher than the stopping length of the electrons with energies of a few tens of keV. Another crucial condition is that the electron beam duration should be sufficiently short, not to exceed more than 10 times the characteristic loading time, which is of the order of a few tens of ps. Although the presented model is limited to monoenergetic electrons and one-dimensional plane geometry, it can be readily generalized to more realistic cases relevant to ICF.

The case presented in Fig. 2 corresponds to the fast electron current of 30 GA/cm^2, which can be generated

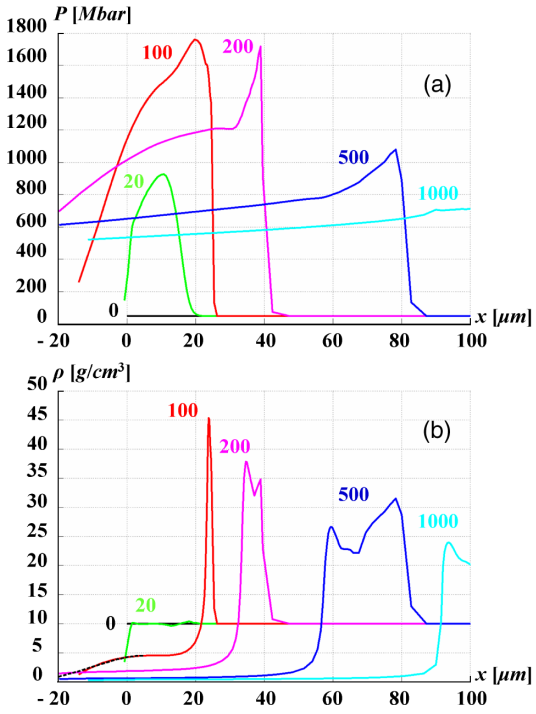

FIG. 3 (color online). Snapshots of distributions of the plasma pressure (a) and the density (b). The numbers near the curves indicate the time in picoseconds. The electron beam energy is 100 keV and the intensity is 10 PW/cm^2. Dashed line in panel b shows the self-similar solution (3).

with high power laser pulses. The numerical simulations of laser plasma interaction [11] predict the efficiency of laser absorption more than 70% with 90% conversion in fast electrons for the laser intensities exceeding 10 PW/cm^2 at the wavelength 0.35 μm. The laser accelerated electrons with energies less than 100 keV could be efficient drivers of strong shocks for ignition of ICF targets and for other high energy density applications. Such drivers could invest about 10% of energy in the shock wave in solids with a pressure amplitude at the level of several hundred Mbar or more.

This work was performed in the framework of the HiPER project EC FP7 No. 211737. It is supported by the EURATOM within the "Keep-in-Touch" activities, the Aquitaine Regional Council, and the Russian Foundation for Basic Research (Project No. 12-02-92101-JF).

*ribeyre@celia.u-bordeaux1.fr

[1] J. Lindl, *Inertial Confinement Fusion: The Quest for Ignition and Energy Gain Using Indirect Drive* (AIP-Press, New York, 1998).
[2] P. P. Volosevich and V. B. Rozanov, JETP Lett. **33**, 17 (1981).
[3] S. Yu. Gus'kov, V. V. Zverev, and V. B. Rozanov, Sov. J. Quantum Electron. **13**, 498 (1983).
[4] R. G. Evans, Laser Part. Beams **1**, 231 (1983); Plasma Phys. Controlled Fusion **28**, 157 (1986).

[5] M. Tabak, J. Hammer, M. E. Glinsky, W. L. Kruer, S. C. Wilks, J. Woodworth, E. M. Campbell, M. D. Perry, and R. J. Mason, Phys. Plasmas **1**, 1626 (1994).
[6] V. A. Scherbakov, Sov. J. Plasma Phys. **9**, 240 (1983).
[7] R. Betti, C. D. Zhou, K. S. Anderson, L. J. Perkins, W. Theobald, and A. A. Solodov, Phys. Rev. Lett. **98**, 155001 (2007).
[8] V. N. Gamezo, A. M. Khokhlov, and E. S. Oran, Phys. Rev. Lett. **92**, 211102 (2004).
[9] V. Bychkov, D. Valiev, and L. E. Eriksson, Phys. Rev. Lett. **101**, 164501 (2008).
[10] O. Klimo, S. Weber, V. T. Tikhonchuk, and J. Limpouch, Plasma Phys. Controlled Fusion **52**, 055013 (2010).
[11] O. Klimo, V. T. Tikhonchuk, X. Ribeyre, G. Schurtz, C. Riconda, S. Weber, and J. Limpouch, Phys. Plasmas **18**, 082709 (2011).
[12] X. Ribeyre, G. Schurtz, M. Lafon, S. Galera, and S. Weber, Plasma Phys. Controlled Fusion **51**, 015013 (2009).
[13] A. V. Gurevich, L. V. Pariiskaya, and L. P. Pitaevskii, Sov. Phys. JETP **22**, 449 (1966).
[14] W. M. Manheimer, D. G. Colombant, and J. H. Gardner, Phys. Fluids **25**, 1644 (1982).
[15] R. Fabbro, C. Max, and E. Fabre, Phys. Fluids **28**, 1463 (1985).
[16] A. R. Bell and M. Tzoufras, Plasma Phys. Controlled Fusion **53**, 045010 (2011).
[17] V. S. Imshennik, Sov. Phys. Dokl. **5**, 263 (1960).
[18] The solution found in Ref. [17] was published recently by R. P. Drake, Phys. Plasmas **18**, 104506 (2011).
[19] P. Mora, Phys. Rev. Lett. **90**, 185002 (2003).
[20] L. D. Landau and E. M. Lifshitz, *Fluids Mechanics* (Pargamon Press, London, 1959).
[21] Here, we consider the cold target as an ideal gas with the polytrope index $5/3$.
[22] J. Breil and P.-H. Maire, J. Comput. Phys. **224**, 785 (2007).
[23] Ph. Nicolaï, J.-L. Feugeas, C. Regan, M. Olazabal-Loumé, J. Breil, B. Dubroca, J.-P. Morreeuw, and V. Tikhonchuk, Phys. Rev. E **84**, 016402 (2011).
[24] B. Dubroca, J.-L. Feugeas, and M. Frank, Eur. Phys. J. D **60**, 301 (2010).